Original paper

Folia Neuropathologica

The use of MR perfusion parameters in differentiation between glioblastoma recurrence and radiation necrosis

Barbara Bobek-Billewicz[1], Sylwia Heinze[2], Aleksandra Awramienko-Wloczek[1], Krzysztof Majchrzak[3], Elzbieta Nowicka[4], Anna Hebda[1]

[1]Department of Radiology, Maria Sklodowska-Curie National Research Institute of Oncology, Gliwice Branch, Poland, [2]Department of Radiology, Maria Sklodowska-Curie National Research Institute of Oncology, Cracow Branch, Poland, [3]Department and Clinical Ward of Neurosurgery, Medical University of Silesia, Sosnowiec, Poland, [4]III[rd] Radiotherapy and Chemotherapy Department, Maria Sklodowska-Curie National Research Institute of Oncology, Gliwice Branch, Poland

Folia Neuropathol 2023; 61 (4): 371-378 *DOI: https://doi.org/10.5114/fn.2023.134180*

Abstract

Introduction: *This study focuses on the challenge of distinguishing between tumour recurrence and radiation necrosis in glioma treatment using magnetic resonance imaging (MRI). Currently, accurate differentiation is possible only through surgical biopsy, which is invasive and may cause additional damage. The study explores non-invasive methods using dynamic susceptibility contrast (DSC) MR perfusion with parameters like relative peak height (rPH) and relative percentage of signal-intensity recovery (rPSR).*

Material and methods: *Among retrospectively evaluated patients (multicentre study) with an initial diagnosis of the primary and secondary brain tumour, 47 met the inclusion criteria and were divided into two groups, the recurrent glioblastoma (GBM) WHO IV group and the radiation necrosis group, based on MRI of the brain. All patients enrolled into the recurrent GBM group had a second surgical intervention.*

Results: *Mean, minimum and maximum rPH values were significantly higher in the recurrent GBM group than in the radiation necrosis group ($p < 0.001$), while rPSR values were lower in the recurrent GBM group than in the radiation necrosis group ($p = 0.011$ and $p = 0.012$).*

Discussion: *This study investigates the use of MR perfusion curve characteristics to differentiate between radiation necrosis and glioblastoma recurrence in post-treatment brain tumours. MR perfusion shows promising potential for distinguishing between the two conditions, but it also has certain limitations. Despite challenges in finding a sufficient cohort size, the study demonstrates significant differences in MR perfusion parameters between radiation necrosis and GBM recurrence.*

Conclusions: *The results demonstrate the potential usefulness of these DSC perfusion parameters in discriminating between glioblastoma recurrence and radiation necrosis.*

Key words: *head, magnetic resonance, radiation necrosis, glioblastoma, magnetic resonance perfusion.*

Introduction

Radiotherapy is one of the main therapeutic methods used after surgery in the glioma treatment, principally in the glioblastoma (GBM). It is well known that it often causes radiation necrosis (RN), the severe type of radiation injury, so the follow up in magnetic resonance imaging (MRI) is required for the evaluation of the therapy. Differentiating between treatment-induced necrosis and tumour recurrence is a crucial challenge in neuro-oncology. Inadequate diagnosis can lead to invasive and hazardous surgical intervention.

Tumour growth is often accompanied by the disruption of the blood-brain barrier (BBB) and a higher

Communicating author:

Sylwia Heinze, PhD, Department of Radiology, Maria Sklodowska-Curie National Research Institute of Oncology, Cracow Branch, Poland, e-mail: sylwia.heinze@onkologia.krakow.pl

cerebral blood volume (CBV) because of the angiogenesis process. This phenomenon is also observed in radiation injury. Both types of lesions appear hyperintense on T2-weighted MR images and strongly enhances after contrast injection, what usually makes the distinction between radiation necrosis and tumour recurrence a diagnostic dilemma as they usually show similar conventional MRI features. Furthermore, a new contrast-enhancing lesion observed on follow-up imaging is often a mixture of necrotic tissue and growing tumour, and this adds to the complexity of lesion characterization. It is essential to be able to determine the aetiology of a lesion observed on follow-up imaging because the management strategies for tumour recurrence and treatment necrosis are different. Tumour pseudoprogression, when lesion increases in size due to treatment and mimics progressive disease, is also a phenomenon that can make proper diagnosis even harder.

Currently, surgical biopsy or resection is the only accurate differentiating method. That option is beneficial for patients with recurrent tumours, however, in cases of radiation necrosis it would lead to further damage to adjacent normal cerebral parenchyma. Therefore, there is significant interest in developing non-invasive methods that could determine whether a contrast enhancement is caused by treatment necrosis or tumour recurrence.

Dynamic susceptibility contrast (DSC) MR perfusion relies on the susceptibility induced signal drop on T2*-weighted sequences caused by gadolinium-based contrast passing through a capillary bed. The hemodynamic parameters of the tissue can be quantified using the relative cerebral blood volume (rCBV), relative peak height (rPH) and relative percentage of signal-intensity recovery (rPSR) [14].

The main goal of our study was to evaluate the usefulness of the two DSC perfusion parameters, rPH and rPSR, to discriminate between glioblastoma recurrence and radiation necrosis.

Material and methods

Patients

We identified and retrospectively evaluated patients with an initial diagnosis of the primary and secondary brain tumour between 8 February 2006, and 15 March 2021. The cohort was divided into two groups, the recurrent GBM WHO IV group and the radiation necrosis group, based on MRI of the brain. The patient had to meet all of the following criteria in order to be included in one of the groups:

The recurrent GBM group (Fig. 1) – the patient underwent the tumour resection and histological findings confirmed the GBM diagnosis; underwent standard GBM treatment according to Stupp protocol (external beam radiation therapy along with chemotherapy followed by adjuvant chemotherapy); a new contrast-enhancing lesion appeared in the brain and DSC MR perfusion was performed during that MR exam; the patient underwent the second tumour resection and subsequent histological findings confirmed the GBM recurrence diagnosis; MR examination following the surgery was performed to confirm the scope of the resection.

The radiation necrosis group (Fig. 2) – the patient underwent the tumour resection and histological findings confirmed the presence of glioma or metastasis; the patient underwent external beam radiation therapy; a new contrast-enhancing lesion appeared in the brain and DSC MR perfusion was performed during that MR exam; the lesion decreased in size or disappeared in the following MR examinations or the patient underwent the second tumour resection with histologically proven radiation necrosis; MR examination following the surgery was performed to confirm the scope of the resection.

- Forty-seven subjects met the inclusion criteria, 23 women and 24 men, mean age 49 ±12 years old. Thirty (64%) patients were included into the recurrent GBM group and 17 (36%) patients were included into the

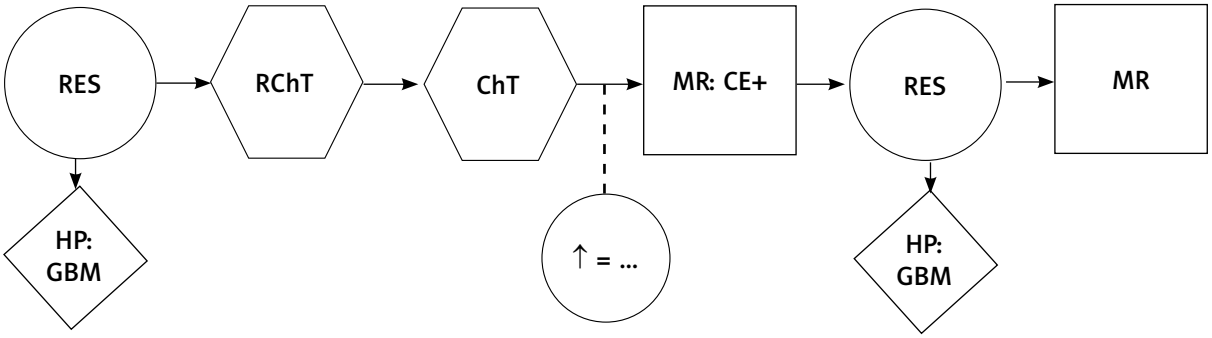

Fig. 1. Recurrent glioblastoma group – inclusion criteria.

radiation necrosis group. All the information about histopathological findings in both groups after the 1st resection is presented in Table I. All patients enrolled into the recurrent GBM group had a second surgical intervention, in the radiation necrosis group only 5/17 (29%) were histopathologically proven cases of necrosis. The remaining 12/17 (71%) were the cases of contrast-enhancing lesions which shrank or disappeared in the follow-up studies.

- Patients were excluded from the study if they did not undergo initial gross total resection or if they were lost to follow-up with lack of a second surgical pathologic verification. All contraindications to MRI examination including implants, cardiac pacemakers or metallic foreign bodies were excluded. We also excluded patients with non-enhancing suspicious lesions.

MR imaging protocol

Images were acquired with one of the following MR scanners: Siemens Magnetom Prisma 3T, Siemens Magnetom Vida 3T, Siemens Magnetom Aera 1,5T, Siemens Magnetom Avanto 1,5T or Philips Achieva 3T. Images on which the analysis was based on were acquired with the following sequences: T2-weighted spin-echo, pre-contrast T1-weighted spin-echo, post-contrast T1-weighted spin-echo and T2*-weighted echo-planar DSC perfusion imaging. Parameters such as the slice thickness (4 mm), the gap between the slices (20%) and the table position were the same in all of the sequences for each patient.

The DSC perfusion imaging sequence comprised 60 acquisitions and the scan was performed before, during and after the bolus injection. At the 10th acquisition the gadolinium-based contrast agent (0.1 mmol/kg of body weight) was injected intravenously at the rate of 6 ml/s and followed immediately with the 30 ml saline flush at the same rate. All injections were performed using an automatic power injector. All axial sections were aligned with pre-contrast T1-weighted images and the entire tumour volume was covered.

Table I. Histopathological findings after the 1st and 2nd resection in both groups

	Histopathological result	WHO grade	Recurrent GBM	Radiation necrosis
1st resection	Glioblastoma	IV	30	4
	Astrocytoma anaplasticum partim granulocellulare	III	–	1
	Astrocytoma anaplasticum	III	–	3
	Astrocytoma fibrillare	II	–	2
	Oligodendroglioma anaplasticum	III	–	2
	Oligoastrocytoma	II	–	1
	Oligoastrocytoma anaplasticum	III	–	1
	Oligoastrocytoma gemistocyticum	II	–	1
	Metastasis	–	–	2

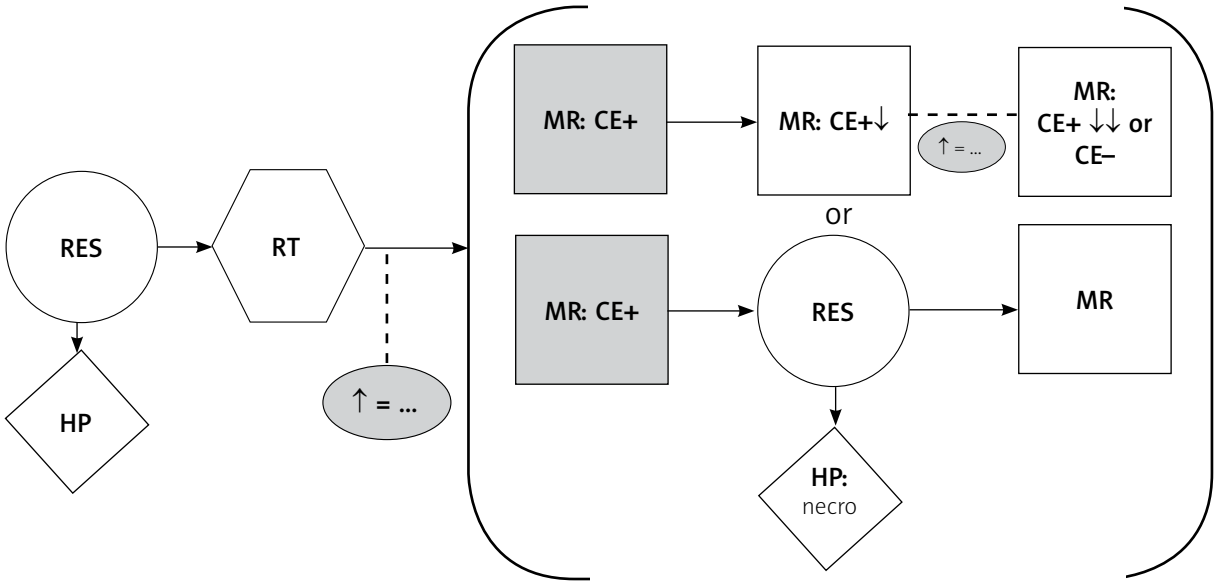

Fig. 2. Radiation necrosis group – inclusion criteria.

Image processing and evaluation

Based on the suitable MR examination, the image processing was performed using commercially available software (syngo.via, Siemens). Before the analysis all images were reviewed in order to check for any artifacts that could spoil the results of the analysis.

The raw DSC perfusion images were used to calculate both the CCBV maps and signal intensity-time curves. During the analysis, the aligned imaging data was used to manually draw three regions of interest (ROIs) on each slice where contrast-enhancing lesion was present. First ROI was drawn around the entire contrast-enhancing lesion, excluding non-contrast-enhancing tissue that might have been located within the lesion area. Second 0.5 cm^2 ROI was drawn around the enhancing part of the lesion with the highest CBV value. The last 1 cm^2 ROI was drawn in the contralateral brain hemisphere normal appearing white matter (NAWM). For each patient the first and the last ROI were manually drawn on the post-contrast T1 image, the second ROI was manually drawn on the CCBV map within the first ROI and all of them were placed also on raw DSC perfusion image.

T2* signal intensity-time curves

The T2* signal intensity-time (SI-time) curves were generated for three ROIs placed on raw DSC perfusion images and based on them the following parameters were calculated: rPH and rPSR. To calculate the values of rPH and rPSR some key points must be defined on T2* SI-time curve – S_0, S_{min} and S_1. S_0 is the signal intensity on the T2* SI-time curve before contrast administration, S_{min} is the minimum signal intensity value on the T2*-curve and S_1 is the post-contrast signal intensity on the T2* SI-time curve. S_1 had to be defined carefully as the contrast recirculation might have appeared after the initial dip [2].

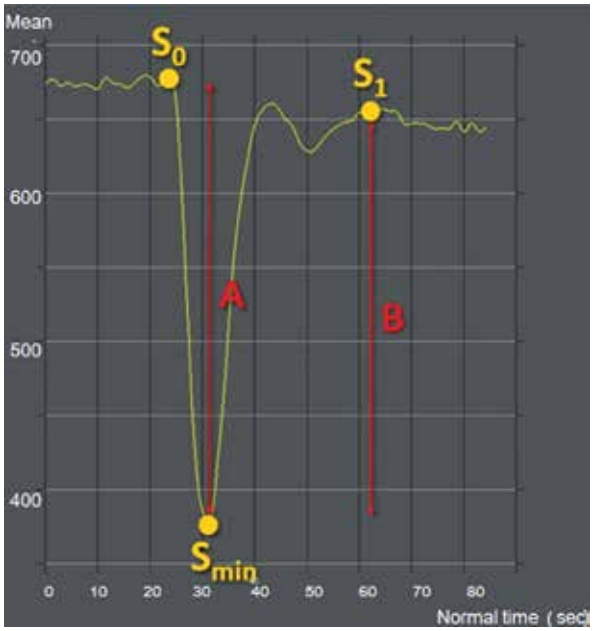

Fig. 3. Signal intensity-time curve for DSC MR perfusion.

Peak height (Fig. 3A) represents the maximal drop of signal intensity during the first pass of contrast agent and it reflects total capillary volume:

$$PH = S_0 - S_{min}$$

then: rPH is the ratio of PH for ROI divided by PH for NAWM and it is defined by the following formula:

$$rPH = \frac{S_{0\,[ROI]} - S_{min\,[ROI]}}{S_{0\,[NAWM]} - S_{min\,[NAWM]}} = \frac{PH_{ROI}}{PH_{NAWM}}$$

Percentage of signal-intensity recovery (Fig. 3) provides information about the tumour capillary permeability, reflects the BBB integrity and contrast agent leakage from tumour capillaries. PSR is the ratio of signal intensity during the recirculation phase divided by its initial value.

$$PSR\,[\%] = \frac{S_1 - S_{min}}{S_0 - S_{min}}$$

then: rPSR is the ratio of PSR for ROI divided by PSR for NAWM and it is defined by the following formula:

$$rPSR\,[\%] = \frac{PSR_{ROI}}{PSR_{NAWM}}$$

Mean and minimum rPH and rPSR were calculated based on ROIs drawn around the entire contrast-enhancing lesion, whereas maximum rPH and rPSR were calculated based on 0.5 cm^2 ROI drawn around the enhancing part of the lesion with the highest CBV value. Examples of measurements and ROIs placement for both radiation necrosis and recurrent glioblastoma can be found on Figures 4 and 5.

Statistical analysis

Statistical analysis was conducted using commercial software Statistica version 12, StatSoft. For each parameter (mean, minimum and maximum rPH and rPSR), the following steps were applied: at first, the Shapiro-Wilk test was applied to determine whether the data fit a normal distribution. Mann-Whitney *U*-test and Student *t*-test were performed to check if

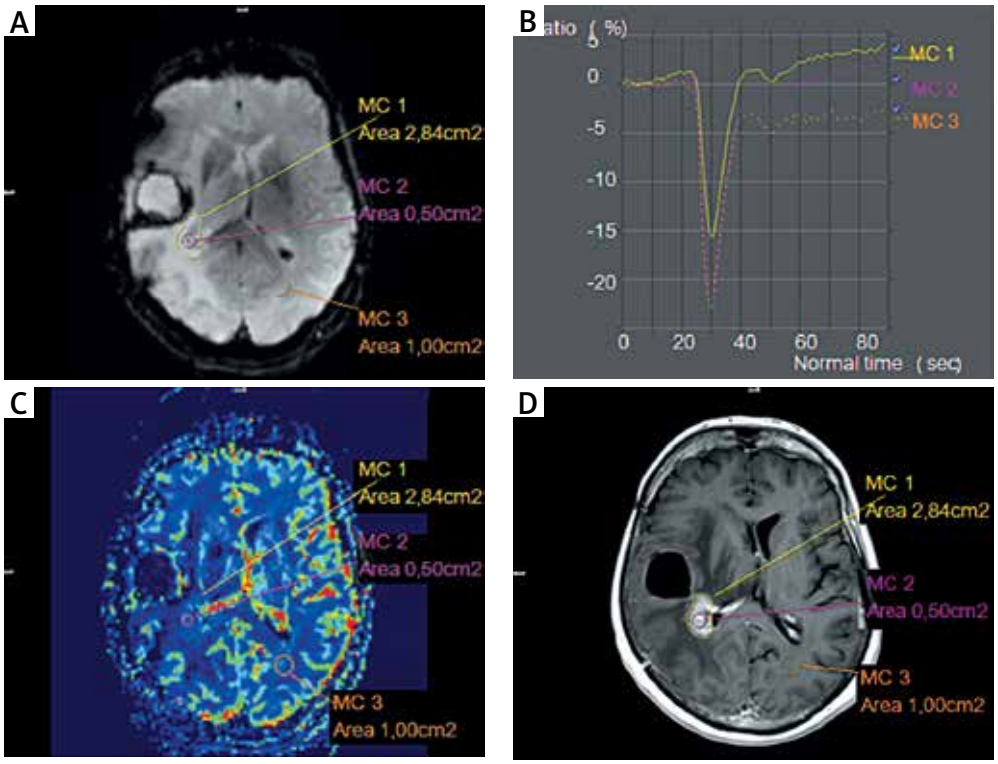

Fig. 4. Example of radiation necrosis: **A**) raw perfusion sequence, **B**) signal intensity-time curves for different ROIs, **C**) relCCBV map with ROIs, **D**) t1 MPRage with contrast and with ROIs.

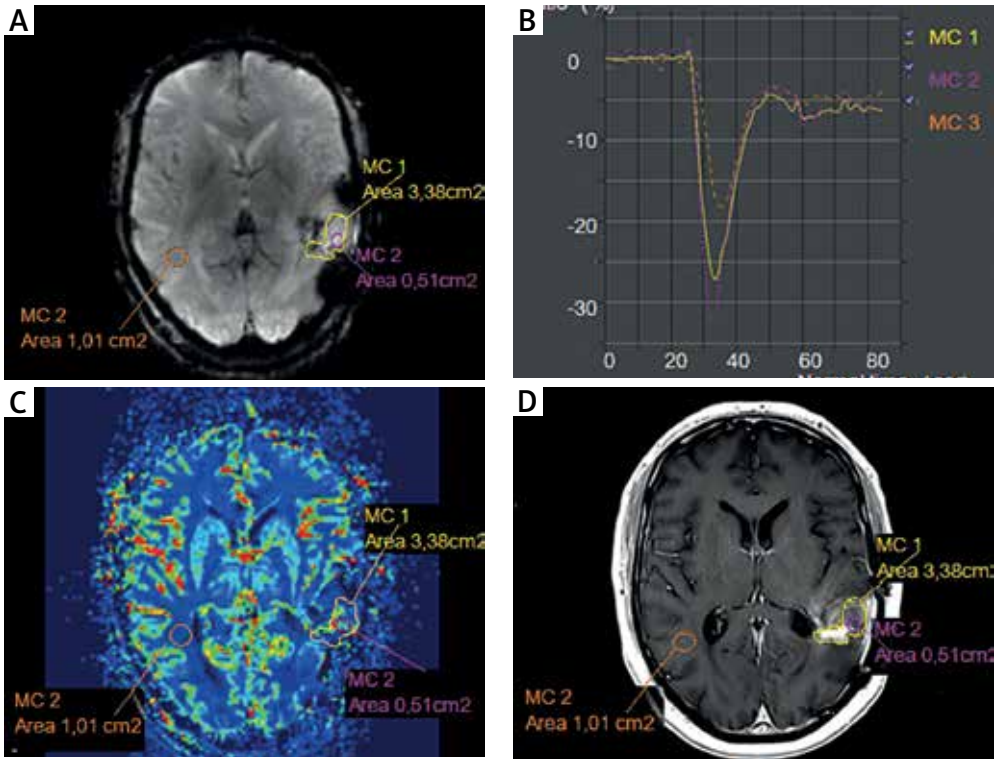

Fig. 5. Example of recurrent glioblastoma: **A**) raw perfusion sequence, **B**) signal intensity-time curves for different ROIs, **C**) relCCBV map with ROIs, **D**) t1 MPRage with contrast and with ROIs.

differences between groups were statistically significant and a p value of less than 0.05 was considered to indicate the significance. Finally, to define cut-off points, ROC analysis was applied and Youden's index was calculated.

Results

Mean, minimum and maximum rPH values were significantly higher in the recurrent GBM group than in the radiation necrosis group ($p < 0.001$), whereas mean and maximum rPSR were significantly lower in the recurrent GBM group than in the radiation necrosis group ($p = 0.011$ and $p = 0.012$, respectively) (Table II). Minimum rPSR is concerned insignificant in terms of GBM recurrence and radiation necrosis differentiation.

Tables III and IV provide information about the results of the whole analysis. Table III comprises general information about the groups and basic statistics, whereas Table IV provides cut-off points for each parameter and summarizes the analysis.

Discussion

Gliomas are the most common primary brain tumours in adults treated with surgical excision followed by radio-chemotherapy [12]. Post-treatment surveillance often involves serial magnetic resonance imaging. The suspicious lesion may represent post-treatment radiation effects such as pseudoprogression, radiation necrosis or tumour recurrence. Damages caused by radiotherapy appear months after the time of the treatment and usually consist of necrosis caused by BBB disruption and radiation-induced demyelination followed by white matter injury. Radiation necrosis most often is visible at the site of the previous tumour [11]. Tumour pseudoprogression, which corresponds to an increase in lesion size related to treatment, which simulates progressive disease mimicking tumour progression on medical imaging is observed after combined chemotherapy and radiotherapy in about 30% of patients. Radiotherapy alone is less likely to result in pseudoprogression, and is only

Table II. For each parameter: median value and lower and upper quartile (in brackets). *P* was established based on the following statistical tests: *Mann-Whitney *U*-test, **Student *t*-test

	rPH			rPSR		
	Mean*	Minimum*	Maximum**	Mean*	Minimum*	Maximum*
Recurrent GBM	2.40 (1.87-2.84)	1.78 (1.38-2.50)	3.88 (2.95-5.64)	107.53 (97.96-123.27)	99.06 (88.03-107.35)	112.79 (105.24-123.67)
Radiation necrosis	0.96 (0.70-1.23)	0.61 (0.53-0.90)	2.00 (1.48-2.52)	129.14 (109.82-139.24)	106.15 (96.63-117.12)	131.23 (120.13-158.84)
P	< 0.001	< 0.001	< 0.001	0.011	0.180	0.012

Table III. Mean values for each parameter ± standard deviation. *P* was established based on the following statistical tests: *Mann-Whitney *U*-test, **Student *t*-test

	rPH			rPSR		
	Mean*	Minimum*	Maximum**	Mean*	Minimum*	Maximum*
Recurrent GBM	2.47 ±0.85	1.92 ±0.74	4.41 ±1.95	110.33 ±17.89	99.73 ±16.62	117.88 ±23.49
Radiation necrosis	1.20 ±0.79	0.89 ±0.66	2.15 ±1.17	133.96 ±40.70	115.38 ±37.96	146.09 ±55.42
P	< 0.001	< 0.001	< 0.001	0.011	0.180	0.012

Table IV. Cut-off values, sensitivity, specificity and area under the curve (AUC) for the parameters that were statistically significant

Parameter	rPH			rPSR	
	Mean	Minimum	Maximum	Mean	Maximum
Cut-off point	1.44	1.04	2.55	112.00	118.10
Sensitivity	96.7	93.3	90.0	70.0	73.3
Specificity	76.5	82.4	76.5	70.6	82.4
AUC	0.87	0.86	0.86	0.73	0.72

observed in about 15% of patients. It appears within 3-6 months of radiotherapy, frequently earlier than adjuvant temozolomide is finished. Unfortunately, interpretation of pseudoprogression as treatment failure can lead to untimely interruption of chemotherapy. Radiation necrosis develops 6 months after radiotherapy and is more severe, typically requiring steroids or surgical intervention [7].

Post-treatment tumour recurrence and radiation necrosis appear similar in conventional MR imaging, however, the proper therapeutic strategy is completely different, so the ability to differentiate between RN and recurrent tumour at the early stage is very important for patients' further therapy [13]. The histopathological characteristics of radiation necrosis include coagulation and liquefaction necrosis in the white matter, with capillary collapse and wall thickening and hyalinization of the vessels [4,16]. Telangiectasia is also reported to be a result of the genesis of collateral blood flow against ischemia caused by the obstruction of small venules and arterioles [1,3]. On the other hand, histological features of recurrent glioblastoma included highly cellularity, absence of perinecrotic pseudopalisading and microvascular proliferation. Other characteristics, such as presence of mitoses and hypertrophic endothelial cells, are consistent with glioblastoma recurrence but not necessarily diagnostic of active high-grade tumour [15]. Up to now, the gold standard to set a proper diagnosis has been stereotactic biopsy. However, this technique carries a certain risk of general anaesthesia side effects, intracranial haemorrhage, infection at the pin site or incision site, as well as sampling error if tumour cells were not included in the biopted samples [17]. Alternative methods for surgical intervention, including MR spectroscopy and positron-emission tomography (PET), allowing for non-invasive differentiation between tumour recurrence from radiation necrosis were considered [5,9,10].

The main goal of the current study was to check the usefulness of MR perfusion curve characteristics as a support to the classification of GBM recurrence versus necrosis. This technique has been described by several authors to be useful in trials to differentiate recurrent tumour from the radiation effect [6,8]. MR perfusion imaging allows measuring vascularity within brain lesions and can be acquired during the same session as conventional MR imaging. The vascularisation of malignant tumour is different from that of radiation necrosis [4]. In this study, DSC MR perfusion was performed in all patients. We considered the parameters rPH and rPSR calculated on data sets obtained with this technique, and we tried to find if there is a cut-off value enabling for differentiation between RN and tumour reccurence (TR).

In the current series, the mean (rec GBM 2.47 ±0.85, RN 1.20 ±0.79), maximum (rec GBM 4.41 ±1.95, RN 2.15 ±1.17), and minimum rPH (rec GBM 1.92 ±0.74, RN 0.89 ±0.66) came in good agreement with values published by Barajas *et al*. [2] where presented rPH values were: mean rec GBM 2.07 ±0.69, RN 1.25 ±0.42, maximum rec GBM 3.09 ±1.38, RN 1.72 ±0.55, and minimum rec GBM 1.31 ±0.60, RN 0.82 ±0.38. However, mean (rec GBM 110.33 ±17.89, RN 133.96 ±40.70), maximum (rec GBM 117.88 ±23.49, RN 146.09 ±55.42), and minimum (rec GBM 99.73 ±16.62, RN 115.38 ±37.96) rPSR differs slightly from published values, where presented rPSR values were: mean rec GBM 80.2 ±10.3, RN 89.3 ±12.4, maximum rec GBM 92.5 ±18.8, RN 100 ±12.0, and minimum rec GBM 68.8 ±10.9, RN 77.2 ±15.0. All the rPSR parameters were slightly higher than those mentioned by Barajas *et al*.

MR perfusion imaging showed some limitations: it is very sensitive to susceptibility artifacts, so its application in patients with haemorrhages, calcifications or surgical clips is limited. DSC MR perfusion is also susceptible to motion artifacts, therefore, patients who were anxious during the examination were often excluded. Other limitations also included contrast-enhancing lesion size as proper analysis requires ones that are big enough (we assumed lesions bigger than 1 cm as sufficient). Only a few radiation necrosis cases were confirmed with the histological result, therefore, in the majority of patients, shrinking contrast-enhancing lesions were observed. However, many patients were lost in follow-up, therefore, even if RN was suspected, patients were not monitored long enough to validate it, hence they had to be excluded from this analysis. That was one of the difficulties that made finding a cohort of satisfactory size challenging and time-consuming.

In conclusion, we showed the presence of significant differences in the parameters determined from the MR perfusion curves. Characteristics of the MR perfusion curve may be helpful in distinguishing radiation necrosis from GBM recurrence.

Disclosure

The authors report no conflict of interest.

References

1. Abed E, Mohammed NH, Elsheshiny AH, Ahmed S, Rashad MH. Relation of post-stroke headachto cerebrovascular pathology and hemodynamics. Folia Neuropathol 2022; 60: 221-227.
2. Barajas RF, Chang JS, Segal MR, Parsa AT, McDermott MW, Berger MS, Cha S. Differentiation of recurrent glioblastoma multiforme from radiation necrosis after external beam radiation therapy with dynamic susceptibility-weighted contrast-enhanced perfusion MR imaging. Radiology 2009; 253: 486-496.

3. Belka C, Budach W, Kortmann RD, Bamberg M. Radiation induced CNS toxicity – molecular and cellular mechanisms. Br J Cancer 2001; 85: 1233-1239.
4. Burger PC, Mahley MS, Dudka L, Vogel FS. The morphologic effects of radiation administered therapeutically for intracranial gliomas: a postmortem study of 25 cases. Cancer 1979; 44: 1256-1272.
5. Chuang MT, Liu YS, Tsai YS, Chen YC, Wang CK. Differentiating radiation-induced necrosis from recurrent brain tumor using MR perfusion and spectroscopy: A meta-analysis. PLoS One 2016; 11: e0141438.
6. Gahramanov S, Muldoon LL, Varallyay CG, Li X, Kraemer DF, Fu R, Hamilton BE, Rooney WD, Neuwelt EA. Pseudoprogression of glioblastoma after chemo- and radiation therapy: diagnosis by using dynamic susceptibility-weighted contrast-enhanced perfusion MR imaging with ferumoxytol versus gadoteridol and correlation with survival. Radiology 2013; 266: 842-852.
7. Hu LS, Eschbacher JM, Heiserman JE, Dueck AC, Shapiro WR, Liu S, Karis JP, Smith KA, Coons SW, Nakaji P, Spetzler RF, Feuerstein BG, Debbins J, Baxter LC. Reevaluating the imaging definition of tumor progression: perfusion MRI quantifies recurrent glioblastoma tumor fraction, pseudoprogression, and radiation necrosis to predict survival. Neuro Oncol 2012; 14: 919-930.
8. Matsusue E, Fink JR, Rockhill JK, Ogawa T, Maravilla KR. Distinction between glioma progression and post-radiation change by combined physiologic MR imaging. Neuroradiology 2010; 52: 297-306.
9. Minamimoto R, Saginoya T, Kondo C, Tomura N, Ito K, Matsuo Y, Matsunaga S, Shuto T, Akabane A, Miyata Y, Sakai S, Kubota K. Differentiation of brain tumor recurrence from post-radiotherapy necrosis with 11C-methionine PET: Visual assessment versus quantitative assessment. PLoS One 2015; 10: e0132515.
10. Soliman HM, ElBeheiry AA, Abdel-Kerim AA, Reda MI, Farhoud AH. Recurrent brain tumor versus radiation necrosis; can dynamic susceptibility contrast (DSC) perfusion magnetic resonance imaging differentiate. Egypt J Radiol Nucl Med (Online) 2018; 49: 719-726.
11. Sugahara T, Korogi Y, Tomiguchi S, Shigematsu Y, Ikushima I, Kira T, Liang L, Ushio Y, Takahashi M. Posttherapeutic intraaxial brain tumor: the value of perfusion-sensitive contrast-enhanced MR imaging for differentiating tumor recurrence from nonneoplastic contrast-enhancing tissue. AJNR Am J Neuroradiol 2000; 21: 901-909.
12. Wan B, Wang S, Tu M, Wu B, Han P, Xu H. The diagnostic performance of perfusion MRI for differentiating glioma recurrence from pseudoprogression: A meta-analysis. Medicine (Baltimore) 2017; 96: e6333.
13. Wang S, Martinez-Lage M, Sakai Y, Chawla S, Kim SG, Alonso-Basanta M, Lustig RA, Brem S, Mohan S, Wolf RL, Desai A, Poptani H. Differentiating tumor progression from pseudoprogression in patients with glioblastomas using diffusion tensor imaging and dynamic susceptibility contrast MRI. AJNR Am J Neuroradiol 2016; 37: 28-36.
14. Welker K, Boxerman J, Kalnin A, Kaufmann T, Shiroishi M, Wintermark M; American Society of Functional Neuroradiology MR Perfusion Standards and Practice Subcommittee of the ASFNR Clinical Practice Committee. ASFNR recommendations for clinical performance of MR dynamic susceptibility contrast perfusion imaging of the brain. AJNR Am J Neuroradiol 2015; 36: E41-51.
15. Woodworth GF, Garzon-Muvdi T, Ye X, Blakeley JO, Weingart JD, Burger PC. Histopathological correlates with survival in reoperated glioblastomas. J Neurooncol 2013; 113: 485-493.
16. Yoshii Y. Pathological review of late cerebral radionecrosis. Brain Tumor Pathol 2008; 25: 51-58.
17. Young RJ, Gupta A, Shah AD, Graber JJ, Chan TA, Zhang Z, Beal K, Omuro AM. MRI perfusion in determining pseudoprogression in patients with glioblastoma. Clin Imaging 2013; 37: 41-49.